THE JOURNAL OF PHYSICAL CHEMISTRY Letters

Letter

pubs.acs.org/JPCL

Controlled Catalytic Properties of Platinum Clusters on Strained Graphene

Gyubong Kim,[†] Yoshiyuki Kawazoe,[‡] and Kwang-Ryeol Lee*[,†]

[†]Computational Science Center, Korea Institute of Science and Technology, Seoul 136-791, Republic of Korea

[‡]Institute for Materials Research, Tohoku University, Aoba-ku, Sendai, 980-8577, Japan

Supporting Information

ABSTRACT: We employed graphene under isotropic strain as the supporting material for Pt clusters (Pt_x, x = 1, 4, or 6) and studied the site-resolved molecular adsorption behaviors of H_2, CO, and OH on the clusters using ab initio calculations. It was shown that the applied strain enhances the binding of the Pt atom or clusters on the graphene, which lowers the average energy of the d electrons (d-band center). However, for the Pt_4 and Pt_6 clusters that form two Pt atomic layers on the graphene, only the d-band center of the bottommost Pt layer can be readily tuned by the external strain on graphene. However, the site-resolved calculations of molecular binding demonstrate that controlling the d-band center of the bottommost Pt atoms can be a substantial factor for all the catalytic activities of the Pt cluster. We also found that the stability of the Pt/graphene system was enhanced by applying strain to the graphene support.

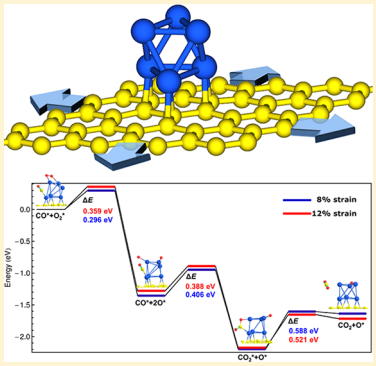

SECTION: Surfaces, Interfaces, Porous Materials, and Catalysis

Pt nanostructures have received particular attention for their excellent catalytic behavior due to their high surface area and exceptional chemical reaction properties.[1−8] An interesting aspect of Pt nanoparticles is that the supporting substrate greatly affects their catalytic properties, which has led to a number of experimental studies on substrate-engineered Pt catalysts. It was shown that the particular defects in graphene and carbon nanotubes (CNTs) improve the catalytic performance of the supported Pt nanoparticles.[9−13] The chemical reactivity and selectivity of Pt nanoparticles also strongly depends on the composition of the supporting substrate.[6,7,14] These experiments showed the versatile catalytic properties of Pt nanoparticles, which could originate from the modification of the electronic structure of Pt by the supporting substrate.[6,7,9−14]

It was demonstrated by first-principles calculations that the average energy of the d electrons, termed the d-band center (ε_d), is strongly correlated with the molecular adsorption strength on the Pt or Pt alloy surfaces.[15,16] These results provided an optimistic prospect that the chemical properties of Pt-based catalysts can be controlled by manipulating a simple parameter, ε_d. Experimentally observed Pt catalytic behaviors, which are influenced by the substrate condition, might be understood in this prospect.[6,7,9−14] However, the catalytic properties of Pt nanostructures are also dependent on the coordination numbers, orbital symmetry, atomic relaxation, and so forth.[17−20] Furthermore, a recent theoretical study showed that the graphene substrate appears to only affect the bottommost (or interfacial) layer of the Pt nanoclusters,[21] implying that the substrate-engineering method might be significantly limited in its ability to control the catalytic properties of the Pt nanoclusters. Although the defects or mechanical strain on graphene is known to modify the chemical properties of supported metal catalysts,[22,23] spatially resolved analysis of the catalytic behavior and corresponding electronic structures of these catalytic systems have yet to be addressed.

In the present work, we investigated the catalytic behavior of Pt nanoclusters on graphene with the isotropic strain, applied uniformly along both of two lattice vectors of graphene. Graphene and CNTs have been widely used as the supporting substrates for metal catalysts because of their excellent structural stability, high accessible area, and chemical versatility.[10−13] In addition, the binding energy of metal atoms or clusters can be tailored by defects or applying strain to the graphene or CNTs, both of which modify the electronic structures of the catalytic metals.[21−25] Graphene under the isotropic strain up to ∼12% was realized either by bending the substrates on which graphene is supported or by pushing a tip of an atomic force microscope on a free-standing graphene, which resulted in many interesting modifications of the electronic structure of the graphene.[26,27] We employed isotropically strained graphene as the supporting substrate for small Pt clusters (Pt_x with x = 1, 4, or 6) as shown in Figure 1 (hereafter, the term "strain" denotes the "isotropic strain" unless specified otherwise). Molecular adsorption of H_2, CO, and OH on the Pt_x/graphene system was investigated for

Received: May 11, 2012
Accepted: July 11, 2012
Published: July 11, 2012

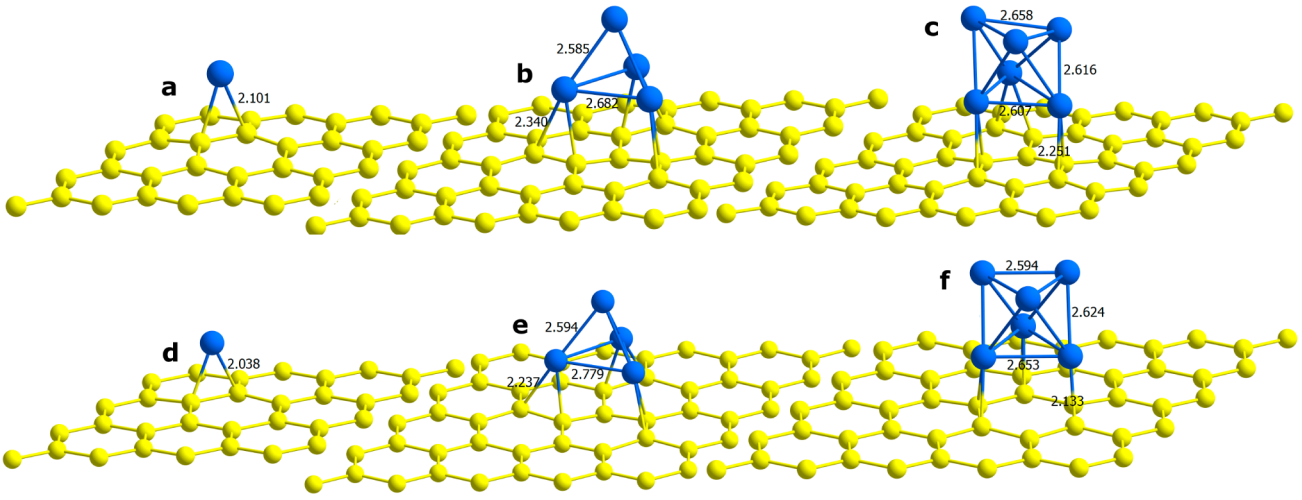

Figure 1. Optimized structures of Pt_1, Pt_4, and Pt_6 binding (from left to right) on pristine (upper panel, a–c) and 12% strained graphene (lower panel, d–f). The blue and yellow balls denote the platinum and carbon atoms, respectively. The changes in Pt–Pt and Pt–graphene bond lengths are at most ~0.1 Å within the strain range of 0–12%.

various values of graphene strain. Site-specific reaction analysis using the molecular binding energy on the Pt nanoclusters demonstrated that the catalytic reactivity of the supported Pt clusters can be effectively controlled by the graphene strain.

All calculations were performed using the first-principles total energy method, as implemented in the Vienna Ab-Initio Simulation Package,[28] and employing the projector augmented wave pseudopotentials.[29] The electron exchange-correlation was treated within the spin-polarized generalized gradient approximation in the form of Perdew–Burke–Ernzerhof-type parametrization.[30] The cutoff energy for the planewave-basis expansion was chosen to be 400 eV, and the atomic relaxation was continued until the Helmann-Feynman forces acting on the atoms were less than 0.02 eV/Å. Graphene supercells with a size of 4 × 4 (for Pt_1) and 5 × 5 (for Pt_4 and Pt_6) were used (see Figure 1), and the distance between graphene layers was set to 20 Å. The Brillouin zone was sampled using Γ-centered 5 × 5 × 1 *k*-point mesh and the electronic levels were convoluted using Gaussian broadening with a width of 0.05 eV.

Figure 1 shows the optimized single Pt atom and Pt nanoclusters on the pristine and strained graphene substrates. Hereafter, we designate the strained graphene as STG(x%) with x being the increase of the lattice constant in % with respect to the equilibrium lattice of graphene. The atomic structures of Pt_x on the strained graphene support showed only slight changes of the bond lengths (at most ~0.1 Å in both Pt–Pt and Pt–C bonds) within the strain range of 0–12%. In general, the reaction of molecular adsorbates on Pt nanoclusters is more complicated than that of solid Pt surfaces, because the reactivity of Pt nanoclusters is also affected by their morphology.[1,5,17−20] However, Pt_x on the strained graphene could be a useful model for investigating the relationship between the binding energy of an absorbing molecule (E_b^{mol}) and ϵ_d because the Pt clusters retain their structures under graphene strain of up to 12% as shown in Figure 1.

We first examined the adsorption of a single Pt atom on the STGs. Figure 2a shows the correlation between the applied strain and the binding energy of Pt (E_b^{Pt}). The E_b^{Pt} on the STG increased as the strain increased. The strong binding of Pt can be an indication of lowered Pt *d* states,[23] which is demonstrated by the strong linear correlation between the graphene strain, E_b^{Pt} and ϵ_d (see Figure 2a): the larger the strain applied on the

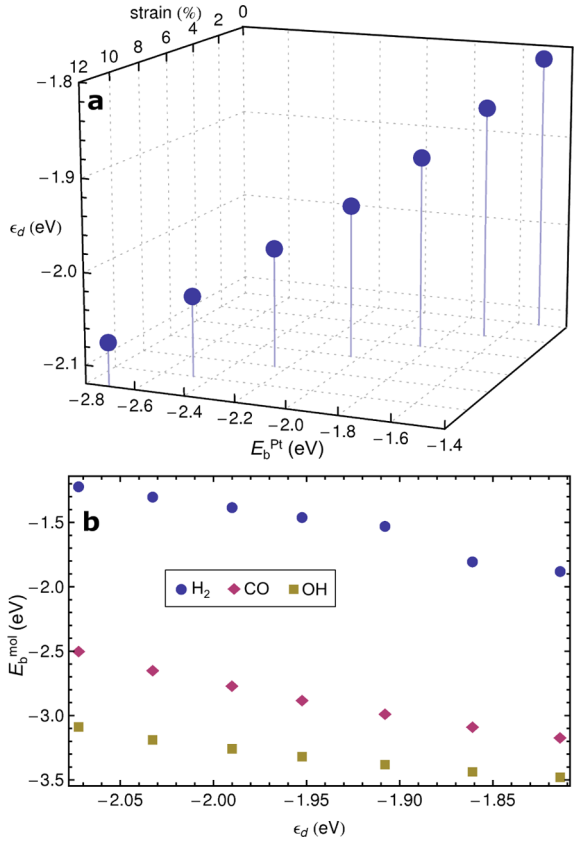

Figure 2. (a) Correlation between the applied strain on graphene, the binding energy of Pt (E_b^{Pt}) and the *d*-band center of Pt (ϵ_d), and (b) molecular binding energies (E_b^{mol}) on the Pt_1/STG system with respect to ϵ_d. Almost linear correlation is noticeable both in (a) and (b).

graphene, the larger the down shift of ϵ_d. Strain-induced modification of the electronic structure of graphene near the Fermi level might be responsible for the enhanced interaction of Pt on the graphene. However, the electronic structure of graphene shows no significant changes with the isotropic strain that maintains all crystal symmetries of graphene.[31] The change of the work function can also play an important role for the

dx.doi.org/10.1021/jz300595g | J. Phys. Chem. Lett. 2012, 3, 1989–1996

metal−graphene interaction by influencing the charge transfer behavior between them.[22,32,33] Choi et al. recently reported that the isotropic strain substantially increases the work function of graphene.[31] However, no significant charge transfer between Pt and graphene was observed in the present work, implying that more elaborate analysis is required to understand the enhanced binding of Pt on the strained graphene. One plausible explanation would be that the change in work function affects the electrostatic potential across the metal−graphene interface, which increases the charge density between Pt and graphene. This explanation can be supported by Figure 3 and Figure S2 (Supporting Information) as will be discussed later.

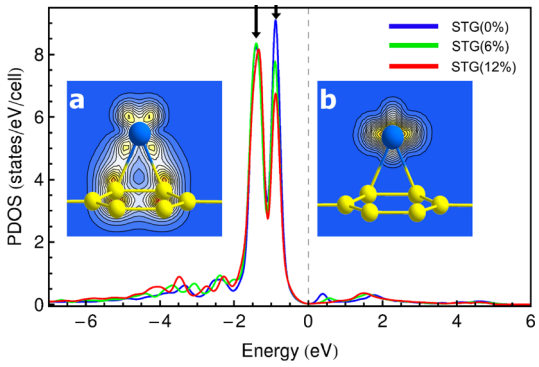

Figure 3. Calculated PDOS projected on *d* orbitals of Pt_1/STG systems (the Fermi level is set at zero energy). It is shown that among two main peaks between −2 and 0 eV (indicated by arrows), the higher-energy peak becomes smaller with the larger strain, while the small peaks are developed below −3 eV. The insets are the charge distributions for (a) the states between −6 and −3 eV and (b) the states between −2 and 0 eV (the contour interval is 0.1 e/Å^3). These charge distributions in insets a and b show the bonding and the nonbonding characters of the corresponding states, respectively.

Figure 2b shows that the E_b^{mol}s of the tested adsorbates (H_2, CO, and OH) on the Pt_1/STG system were strongly dependent on the ε_d tuned by the graphene strain (see Figure S1 for the calculated configurations of molecular binding on Pt_1/STG). This indicates that the catalytic behavior of a Pt atom on graphene can be controlled effectively by the strain applied to the graphene substrate. In contrast to the *d* states of solid Pt surfaces, those of a single atom or small clusters are well localized and possess rather discrete energy profiles. In those cases, it is possible that some particular *d* orbitals dominate the interactions with absorbates. However, the observed strong correlation between ε_d and E_b^{mol} (Figure 2b) indicates that ε_d is still a factor that is responsible for determining the E_b^{mol} of the Pt_1/STG system.

For metal/graphene complex cases, the charge transfer from metal to graphene is generally regarded as a key factor to affect the chemical properties of the supported metal atom or the cluster.[22,24,34,35] For example, Zhou et al. reported that such charge transfer significantly promotes the CO oxidation on the Au/graphene system.[22] However, the electronic structures in the Pt_1/STG system showed that the chemical properties of Pt can vary without significant charge transfer to graphene. Figure 3 shows the partial density of states (PDOS) projected on *d* orbitals of the Pt_1/STG system for various values of the graphene strain. Inset a is the charge distribution for the states in the region from −3 to −6 eV, while inset b represents those in the region from 0 to −2 eV. The charge distribution in inset a may show that the low energy peak between −3 and −6 eV are the bonding states between Pt *d* and graphene π orbitals (PDOS of Pt-bonded carbon atoms are shown in Figure S2). On the other hand, inset b shows that the large peaks between 0 to −2 eV are the nonbonding states of Pt *d* orbitals. As shown here, there is no clear sign of charge transfer from Pt *d* orbitals to graphene as the main peaks between −2 and 0 eV (indicated by arrows) in Figure 3 lie at the same energy level below the Fermi level regardless of the applied strain. The number of Pt *d* electrons differed by only about 0.05 electrons between STG(0%) and STG(12%). PDOS of the strained graphene (not shown here) also indicated no charge transfer from Pt to graphene. However, the higher-energy peak among two main peaks became smaller with the applied strain, while the small and broad peaks below −3 eV increased by the coupling with the graphene π states. This analysis showed that the electrons transferred within the Pt *d* states from the high-energy nonbonding states to the low-energy bonding states under the larger grapheme strain, resulting in down-shift of ε_d shown in Figure 2a.

The dependence shown in Figure 2 calculated for the single atom case should be valid for small clusters with a few Pt atoms because a Pt cluster composed of less than 10 atoms tends to form a planar structure[36] where all the constituent Pt atoms can interact directly with the substrate. In the case of multilayered Pt clusters, it was shown that ε_d of the Pt atoms at the interface between the cluster and the graphene was distinguishably down-shifted.[21] However, those of the other Pt atoms are almost unchanged.[21] This may suggest that the catalytic behavior of only the Pt atoms at the interface is largely affected by the substrate modulation, but the molecular interaction of the whole Pt cluster is less affected by the substrate modulation. It is thus necessary to examine the effect of the graphene strain on the catalytic property of Pt clusters in site-specific details.

We employed Pt_4/STG and Pt_6/STG structures consisting of two Pt atomic layers to examine the catalytic properties of the Pt nanoclusters on the STG (see Figure 1). Two atomic layer models with a small number of Pt atoms were used in the present work for computational convenience. However, two such Pt atomic layers would be sufficient to represent the multilayered Pt nanoclusters since the graphene substrate modifies ε_d of only the bottommost interfacial layer of the Pt nanoclusters.[21] Figure 4 shows the dependence of ε_d on the graphene strain for the upper or the lower (interfacial) Pt atoms. The insets in Figure 4 show that the binding energy of the Pt nanoclusters (E_b^{Pt}) increased with the graphene strain, as was also the case for a single Pt atom (see Figure 2a). In both Pt_4/STG and Pt_6/STG systems, ε_d of the interfacial Pt atoms exhibited the same dependence on the graphene strain as that of the Pt_1/STG system: the larger the graphene strain, the lower the ε_d. On the other hand, the ε_d of the upper Pt atoms showed a different behavior for these two cluster sizes. For the Pt_4 cluster, the correlation between the ε_d and the graphene strain is opposite to that of the Pt_1/STG system, and that of the interfacial Pt atoms: ε_d became higher with increased graphene strain. For the Pt_6 cluster, ε_d of upper Pt atoms showed insignificant variation (approximately 0.03 eV) in the present strain range.

Although the electronic structure of a supported Pt nanocluster is a consequence of the complex state coupling between the Pt atoms and the substrate, variation of the interatomic distance between Pt atoms may be a measure of the ε_d value.[15] Figure 1b,e for the Pt_4/STG system shows that the

dx.doi.org/10.1021/jz300595g | J. Phys. Chem. Lett. 2012, 3, 1989−1996

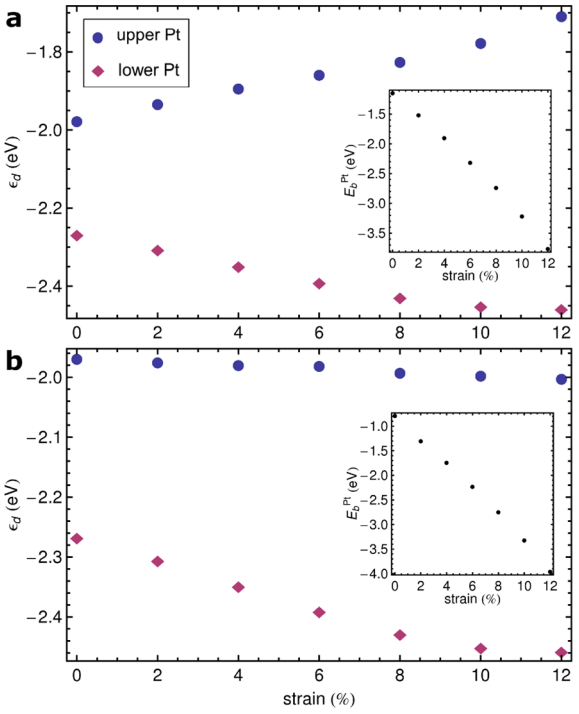

Figure 4. Correlation between the graphene strain and ε_d for (a) Pt_4 and (b) Pt_6 on STG. The insets are the binding energies of the Pt clusters (E_b^{Pt}) with respect to the applied graphene strain. Similar to the Pt_1/STG case (see Figure 2a), the linear relation between the strain and E_b^{Pt} is noticeable for both Pt clusters.

bond length between the upper and the lower Pt atoms increased from 2.585 Å to 2.594 Å as the strain is increased in the graphene, which is associated with higher values of ε_d for the upper Pt atom with increased strain. This is because the lower Pt atoms with the lower ε_d tend to weakly bind the upper Pt atom. For the Pt_6/STG system, the bonding states among the upper Pt atoms should also be involved in determining the ε_d. As shown in Figure 1c,f, increased graphene strain increased the bond length between the upper and the interfacial Pt atoms. On the other hand, the bond lengths between the upper Pt atoms are decreased from 2.658 Å to 2.594 Å due to stabilization of the valence *d* states of the upper Pt atoms. This bonding feature of the Pt clusters may result in moderate variation of ε_d for the upper Pt atoms, depending on the graphene strain.

In the present work, the adsorption of OH and CO on the Pt_4/STG and Pt_6/STG systems was examined. Figure 5 shows the optimized structures of OH adsorbed on Pt_4/STG and Pt_6/STG systems with the strain on graphene being 12%. Commonly, the strongest adsorption centers for a Pt nanocluster or an irregular surface are the sites of low coordination number (e.g., edges, protruding sites) or of high ε_d.[17,19,20] Figure 5a,c also shows that the primary OH adsorption sites in the Pt_4/STG and Pt_6/STG systems were the upper Pt atom sites. It is noted in Figure 4 that these Pt atoms have higher ε_d than the interfacial Pt atoms. Once these preferred adsorption centers of the upper Pt atoms are occupied, the additional OH molecules adsorb on the interfacial Pt atoms as shown in Figure 5b,d. The OH adsorption geometries of Pt_4/STG and Pt_6/STG are all similar in the graphene strain range of 4 to 12%, which will facilitate investigation on OH adsorption in relation to ε_d. For the small strain cases, up to STG(2%), we found that the Pt clusters were separated from the STG at high OH coverage. Such destabilization of the catalyst structure causes a significant loss of catalytic performance.[37,38] However, the Pt nanoclusters was still bound to STG(≥4%) at high OH coverage. This result shows that catalyst degradation can be suppressed by applying strain on the graphene support. The CO binding properties on Pt_4/STG and Pt_6/STG systems were, overall, similar to those of

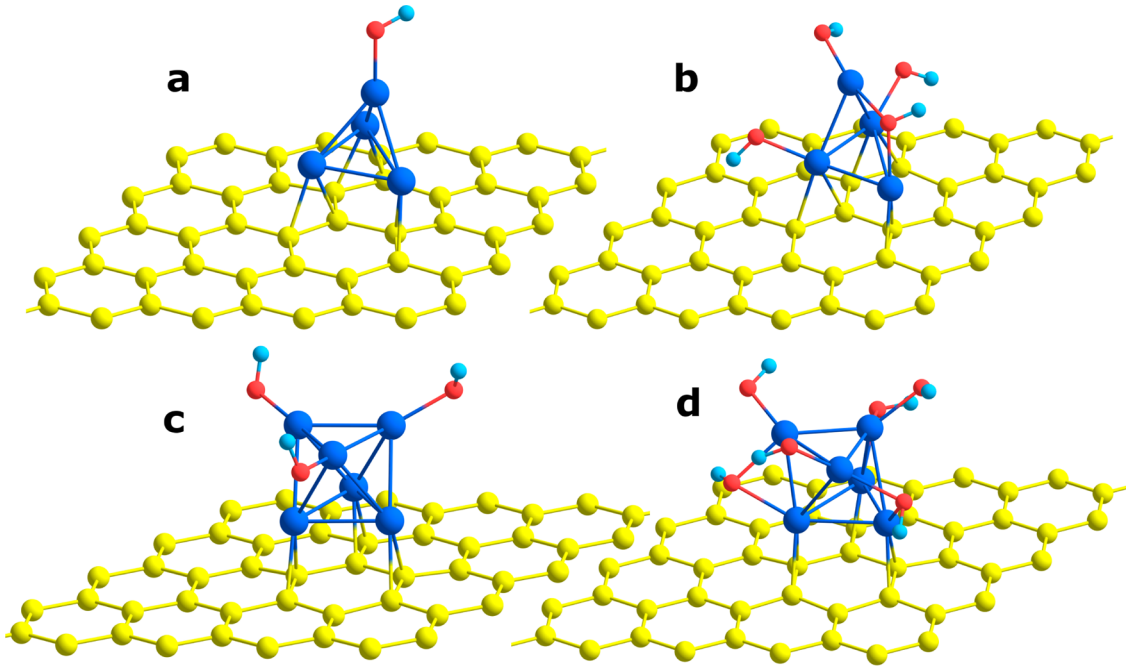

Figure 5. Optimized configurations of OH molecules binding on (a,b) Pt_4/STG(12%) and (c,d) Pt_6/STG(12%). The small cyan and red balls denote the hydrogen and oxygen atoms, respectively. OH tends to bind on the upper Pt atom sites at the lower coverage (a and c), but the lower Pt atom sites also take part in OH binding at the higher coverage (b and d).

dx.doi.org/10.1021/jz300595g | *J. Phys. Chem. Lett.* 2012, 3, 1989–1996

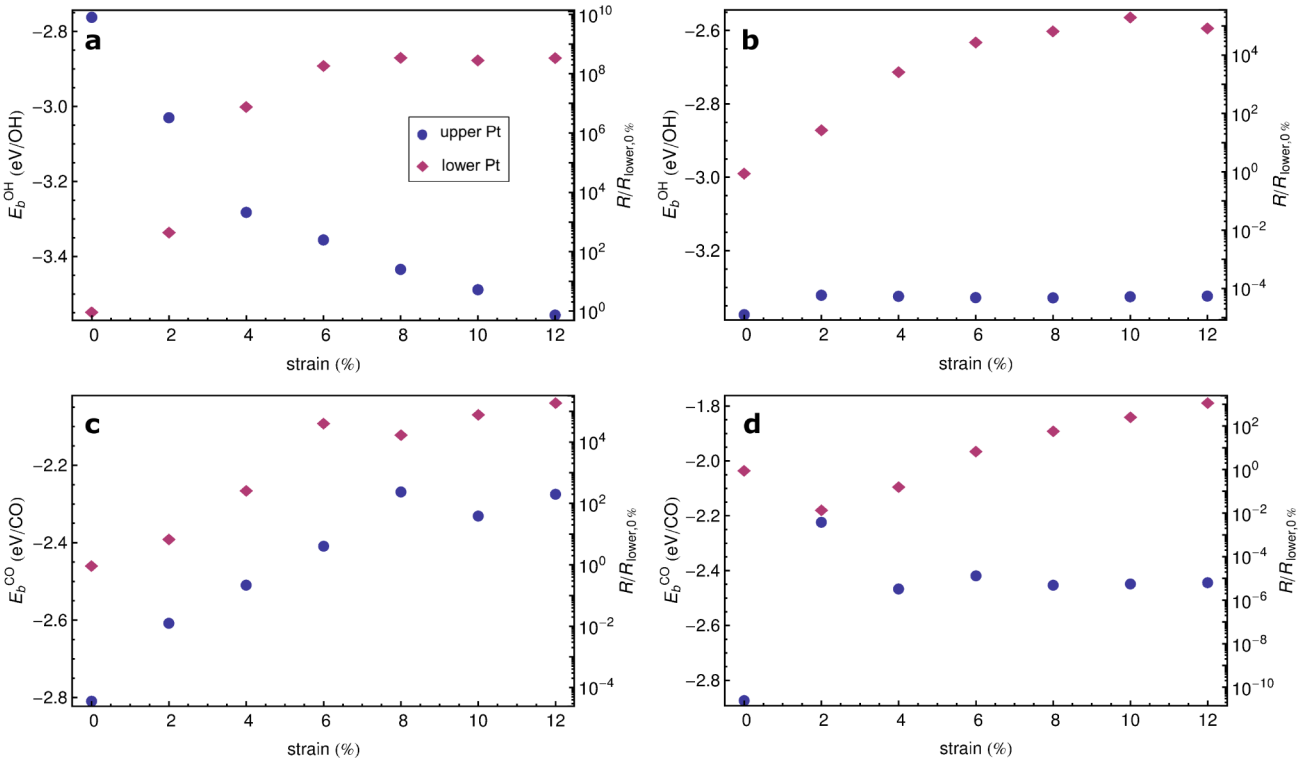

Figure 6. Primary E_b^{mol}'s on the upper Pt atoms and the following E_b^{mols}'s on the lower Pt atoms with respect to the graphene strain in (a,c) Pt_4/STG and (b,d) Pt_6/STG. The upper (a,b) and lower panels (c,d) show the results of OH and CO binding, respectively. Each data point represents the averaged E_b^{mol}'s on the corresponding Pt sites indicated by the legend. These data points can also express the desorption rate $R_{site,\,x\%} \propto \exp(E_b^{mol}/k_BT)$ in log scale (the right vertical axes). Here temperature T is set to 400 K, and R is shown as the proportional value to $R_{lower,0\%}$.

the OH binding cases. The only difference is that, at high CO coverage, the larger graphene strain (≥8% for Pt_4 and ≥6% for Pt_6) is required for Pt clusters to remain attached on STG.

Figure 6 shows the relation between the graphene strain and E_b^{mol} for the upper and the lower Pt sites of the Pt_4/STG and Pt_6/STG systems. First, the E_b^{OH}'s of the lower Pt sites in both Pt clusters became smaller with the graphene strain, i.e., the E_b^{OH} points increase in energy with the strain as shown in Figure 6a,b. This indicates that E_b^{OH} of the interfacial Pt sites can be well controlled by the graphene strain, which leads to the similar relation between the strain, ε_d and E_b^{OH} to the case of a single Pt atom. However, the E_b^{OH} of the upper Pt sites did not consistently depend on the graphene strain. The E_b^{OH} of the upper Pt sites in Pt_4 was enhanced by the graphene strain, whereas that in Pt_6 slightly decreased in the presented strain range. It can easily be observed that all the E_b^{OH} trends for the upper and lower Pt sites are qualitatively coincident with the variation of ε_d (see Figure 4), i.e., the higher the ε_d, the larger the E_b^{OH}. For CO adsorption, a similar relationship is applied except for the upper site in Pt_4/STG. As shown in Figure 6c, E_b^{CO} on the upper site of Pt_4/STG became smaller with the graphene strain when the strain was less than 8%. This is in contrast to that of E_b^{OH}, which might be associated with the stability of the Pt clusters on the STGs upon CO absorption. Even the adsorption of a single CO molecule on Pt_4 can significantly affect the bonding condition between Pt_4 and STG in the strain range of ≤6% (see Figure S3). Such a structural instability may invalidate the simple relationship between ε_d and E_b^{CO}. These results reflect that ε_d and E_b^{mol} of interfacial Pt sites are consistently affected by the graphene strain. However, different behaviors between Pt atoms in different layers make it difficult to understand the catalytic behavior of whole Pt nanoclusters.

The actual catalytic reactions consist of a number of elementary adsorption/desorption steps whose energetics are related to the catalytic reactivity. For an elementary reaction step, the reaction rate is proportional to $\exp(-\Delta E/k_BT)$, where ΔE is the activation energy barrier. By means of the Brønsted–Evans–Polanyi (BEP) relation, ΔE can be described as a linear function of E_b^{mol}'s.[39−42] Therefore, the value of $\exp(E_b^{mol}/k_BT)$ would provide a preliminary estimation for the reaction rate of the reactant desorption processes, as scaled in the right axis of Figure 6. As shown in Figure 6a,b (for STG(≥4%)), E_b^{OH} on the upper Pt sites are larger than that on the lower (interfacial) Pt sites by several hundreds of meV. The small difference in the E_b^{OH} between the Pt sites will significantly affect the desorption rate $R_{site,x\%}$ that is exponentially dependent on E_b^{mol}. [Here, the subscripts "*site*" and "*x*" are, respectively, the molecular adsorption sites (upper or lower Pt) and the amount of the graphene strain.] For example, $R_{lower,12\%}$ is about 10^8 times larger than $R_{upper,12\%}$ at 400K for both Pt_4/STG and Pt_6/STG. In the cases of CO binding, the difference in the reaction rate was also significant when the catalysts are stable [for STG(≥8%)], i.e., 10^3 $R_{upper} \sim R_{lower}$ for Pt_4/STG and 10^8 $R_{upper,12\%} \sim R_{lower,12\%}$ for Pt_6/STG. It is thus expected that, for a reaction whose rate-determining step is the desorption of reactants, the interfacial Pt sites will dominate the catalytic reactivity of the Pt clusters, where ε_d can be readily tuned by STG.

As a more detailed test for the catalytic reaction on the Pt/STG systems, we calculated the energy barrier (ΔE) of the reactions involved in the CO oxidation on Pt_6/STG(8 and 12%). We note that CO oxidation is widely considered as a

dx.doi.org/10.1021/jz300595g | J. Phys. Chem. Lett. 2012, 3, 1989−1996

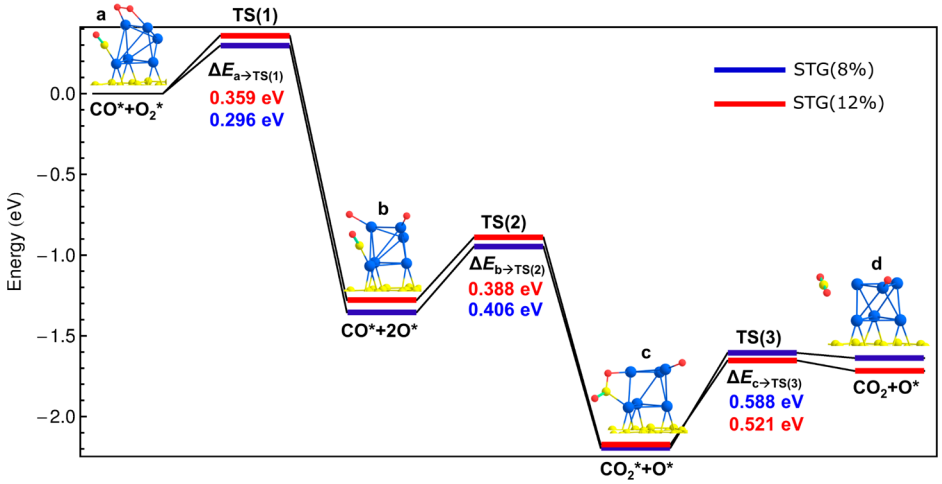

Figure 7. Energy diagrams of CO oxidation on Pt_6/STG(8%) and Pt_6/STG(12%), and (a)-(d) the optimized geometry of each reaction step. Here the energies are relative to that of structure (a). The energy barriers (ΔE) between the elementary steps are shown below the corresponding transition states (TS).

prototype reaction consisting of relatively simple reaction steps.[43] The following three reaction steps were considered in this calculation:

$$CO^* + O_2^* \rightarrow CO^* + 2O^* \quad (1)$$

$$CO^* + 2O^* \rightarrow CO_2^* + O^* \quad (2)$$

$$CO_2^* + O^* \rightarrow CO_2 + O^* \quad (3)$$

where "*" denotes the adsorption state of reactants. CO and O_2 binding sites are chosen to be the lower and upper Pt sites, respectively (see Figure 7a). We chose such CO and O_2 binding geometry by considering the following: The dissociative E_b of O_2 in the reaction 1 should be larger for the upper Pt sites than for the lower Pt sites because the upper Pt sites possess the higher ε_d (see Figure 4). Thus ΔE of O_2 dissociation will be lower at the upper Pt sites based on the BEP relation,[39−42] and the equilibrium coverage of oxygen atoms should also be higher for the upper Pt sites. On the other hand, since reactions 2 and 3 (formation and desorption of CO_2, respectively) are related to destabilization of the bond between CO and Pt, their reaction rates will be much higher for the lower Pt sites than for the upper Pt sites. With these reasons taken into account, the structure shown in Figure 7a could be a rational choice for the representative CO oxidation on the Pt_6/STG system. Since there was no energy barrier for binding of CO or O_2 on Pt, we omitted these molecular binding steps. ΔE for each transition state (TS) is calculated using the nudged elastic band method.[44] Figure 7 shows the energy diagrams of CO oxidation with the optimized atomic configuration of each reaction step. ΔE for O_2 dissociation (reaction 1) is about 63 meV higher for Pt_6/STG(12%) (see TS(1) in Figure 7). But for TS(2) and TS(3) in Figure 7, ΔE values are lower for Pt_6/STG(12%) by 18 and 67 meV, respectively. As TS(3) shows the highest ΔE, the reaction 3 should be the rate-determining step for the CO oxidation reaction. One interesting observation here is that the ΔE values highly depend on the energy gain by the reaction, consistent with the BEP relation:[39−42] the larger the energy gain by the next reaction step, the smaller the value of ΔE. For example, ΔE of TS(1) is smaller for Pt_6/STG(8%) than for Pt_6/STG(12%) as the energy gain by the reaction 1 is larger for Pt_6/STG(8%). The lower ΔEs of TS(2) and TS(3) for Pt_6/STG(12%) can be understood in the same manner, which originate from the weak reactant binding on the lower Pt sites. As the reaction 3 was found to be the rate-determining step, this calculation eventually demonstrated that the graphene strain improved the CO oxidation activity of the Pt cluster by lowering the ε_d of the interfacial Pt sites.

In summary, we investigated the site-resolved catalytic behaviors of Pt nanoclusters on isotropically strained graphene. The estimation of molecular desorption rates indicated that the catalytic reaction on the interfacial Pt site can dominate the catalytic activity of the whole Pt nanoclusters, although the strong correlation between the graphene strain, ε_d and E_b^{mol} is obtained only on the graphene-bonded Pt atoms of the Pt nanoclusters. The strain enhances the binding of the Pt clusters to the graphene, resulting in a lower d band center (ε_d) of interfacial Pt and smaller adsorption energy (E_b^{mol}) of H_2, CO, and OH molecules. A detailed calculation of CO oxidation also supported that the catalytic activity of the Pt/STG system can be controlled by the graphene strain. It was also observed that the Pt clusters were more sustainable on the strained graphene at high adsorbate coverage, which will suppress the degradation of Pt catalyst. These results show that applying a mechanical strain on the graphene support is a promising approach to control the catalytic performance of Pt nanoclusters with improved stability. We also believe that the presented substrate-engineered Pt electronic structures and the molecular adsorption properties will provide a theoretical template for further studies on the catalytic properties of Pt nanostructures.

■ ASSOCIATED CONTENT

Supporting Information

Geometries of H_2, CO, and OH adsorption on Pt_1/STG systems. PDOS of an isolated Pt atom and a graphene-bound Pt atom. Geometries of CO adsorption on the top site of Pt_4/STG systems. This material is available free of charge via the Internet at http://pubs.acs.org.

■ AUTHOR INFORMATION

Corresponding Author

*E-mail: krlee@kist.re.kr; phone: +82-2-958-5494; FAX: +82-2-958-5509.

Notes

The authors declare no competing financial interest.

■ ACKNOWLEDGMENTS

This research was financially supported by the Converging Research Center Program through the MEST (Grant No. 2011K000624) and KIST core capability enhancement program (2E22790). The authors gratefully acknowledge that the SR11000 supercomputing resources of the Center for Computational Materials Science, Institute for Materials Research, Tohoku University, was provided for the present work under the collaboration program of Virtual Organization of Asian Consortium on Computational Materials Science (ACCMS-VO).

■ REFERENCES

(1) Yamamoto, K.; Imaoka, T.; Chun, W.-J.; Enoki, O.; Katoh, H.; Takenaga, M.; Sonoi, A. Size-Specific Catalytic Activity of Platinum Clusters Enhances Oxygen Reduction Reactions. *Nat. Chem.* **2009**, *1*, 397.

(2) Gasteiger, H. A.; Markovic, N. M. Just a Dream—or Future Reality? *Science* **2009**, *324*, 48.

(3) Joo, S. H.; Park, J. Y.; Tsung, C.-K.; Yamada, Y.; Yang, P.; Somorjai, G. A. Thermally Stable Pt/Mesoporous Silica Core−Shell Nanocatalysts for High-Temperature Reactions. *Nat. Mater.* **2009**, *8*, 126.

(4) Tsung, C.-K.; Kuhn, J. N.; Huang, W.; Aliaga, C.; Hung, L.-I.; Somorjai, G. A.; Yang, P. Sub-10 nm Platinum Nanocrystals with Size and Shape Control: Catalytic Study for Ethylene and Pyrrole Hydrogenation. *J. Am. Chem. Soc.* **2009**, *131*, 5816.

(5) Schmidt, E.; Vargas, A.; Mallat, T.; Baiker, A. Shape-Selective Enantioselective Hydrogenation on Pt Nanoparticles. *J. Am. Chem. Soc.* **2009**, *131*, 12358.

(6) Vajda, S.; Pellin, M. J.; Greeley, J. P.; Marshall, C. L.; Curtiss, L. A.; Ballentine, G. A.; Elam, J.; Catillon-Mucherie, S.; Redfern, P. C.; Mehmood, F.; et al. Subnanometre Platinum Clusters as Highly Active and Selective Catalysts for the Oxidative Dehydrogenation of Propane. *Nat. Mater.* **2009**, *8*, 213.

(7) Vayssilov, G. N.; Lykhach, Y.; Migani, A.; Staudt, T.; Petrova, Galina P.; Tsud, N.; Skála, T.; Bruix, A.; Illas, F.; Prince, K. C.; et al. Support Nanostructure Boosts Oxygen Transfer to Catalytically Active Platinum Nanoparticles. *Nat. Mater.* **2011**, *10*, 310.

(8) Qiao, B.; Wang, A.; Yang, X.; Allard, L. F.; Jiang, Z.; Cui, Y.; Liu, J.; Li, J.; Zhang, T. Single-Atom Catalysis of COoxidation Using Pt_1/FeOx. *Nat. Chem.* **2011**, *3*, 634.

(9) Kondo, T.; Izumi, K.-i.; Watahiki, K.; Iwasaki, Y.; Suzuki, T.; Nakamura, J. Promoted Catalytic Activity of a Platinum Monolayer Cluster on Graphite. *J. Phys. Chem. C* **2008**, *112*, 15607.

(10) Centi, G.; Gangeri, M.; Fiorello, M.; Perathoner, S.; Amadou, J.; Bégin, D.; Ledoux, M. J.; Pham-Huu, C.; Schuster, M. E.; Su, D. S.; et al. The Role of Mechanically Induced Defects in Carbon Nanotubes to Modify the Properties of Electrodes for PEM Fuel Cell. *Catal. Today* **2009**, *147*, 287.

(11) Zhou, Y.; Pasquarelli, R.; Holme, T.; Berry, J.; Ginleyc, D.; O'Hayre, R. Improving PEM Fuel Cell Catalyst Activity and Durability Using Nitrogen-Doped Carbon Supports: Observations from Model Pt/HOPG Systems. *J. Mater. Chem.* **2009**, *19*, 7781.

(12) Seger, B.; Kamat, P. V. Electrocatalytically Active Graphene-Platinum Nanocomposites. Role of 2-D Carbon Support in PEM Fuel Cells. *J. Phys. Chem. C* **2009**, *113*, 7990.

(13) Zhou, Y.; Holme, T.; Berry, J.; Ohno, T. R.; Ginley, D.; O'Hayre, R. Dopant-Induced Electronic Structure Modification of HOPG Surfaces: Implications for High Activity Fuel Cell Catalysts. *J. Phys. Chem. C* **2010**, *114*, 506.

(14) Pietrowski, M.; Wojciechowska, M. The Origin of Increased Chemoselectivity of Platinum Supported on Magnesium Fluoride in the Hydrogenation of Chloronitrobenzene. *Catal. Today* **2011**, *169*, 217.

(15) Kitchin, J. R.; Nørskov, J. K.; Barteau, M. A.; Chen, J. G. Modification of the Surface Electronic and Chemical Properties of Pt(111) by Subsurface 3d Transition Metals. *J. Chem. Phys.* **2004**, *120*, 10240.

(16) Pašti, I.; Mentus, S. DFT Study of Adsorption of Hydrogen and Carbon Monoxide on Pt_xBi_{1-x}/Pt(111) Bimetallic Overlayers: Correlation to Surface Electronic Properties. *Phys. Chem. Chem. Phys.* **2009**, *11*, 6225.

(17) Han, B. C.; Miranda, C. R.; Ceder, G. Effect of Particle Size and Surface Structure on Adsorption of O and OH on Platinum Nanoparticles: A First-Principles Study. *Phys. Rev. B* **2008**, *77*, 075410.

(18) Xu, Y.; Getman, R. B.; Shelton, W. A.; Schneider, W. F. A First-Principles Investigation of the Effect of Pt Cluster Size on CO and NO Oxidation Intermediates and Energetics. *Phys. Chem. Chem. Phys.* **2008**, *10*, 6009.

(19) Wang, L.; Roudgar, A.; Eikerling, M. *Ab Initio* Study of Stability and Site-Specific Oxygen Adsorption Energies of Pt Nanoparticles. *J. Phys. Chem. C* **2009**, *113*, 17989.

(20) Chang, L. Y.; Barnard, A. S.; Gontard, L. C.; Dunin-Borkowski, R. E. Resolving the Structure of Active Sites on Platinum Catalytic Nanoparticles. *Nano Lett.* **2010**, *10*, 3073.

(21) Jinnouchi, R.; Toyoda, E.; Hatanaka, T.; Morimoto, Y. First Principles Calculations on Site-Dependent Dissolution Potentials of Supported and Unsupported Pt Particles. *J. Phys. Chem. C* **2010**, *114*, 17557.

(22) Zhou, M.; Zhang, A.; Dai, Z.; Feng, Y. P.; Zhang, C. Strain-Enhanced Stabilization and Catalytic Activity of Metal Nanoclusters on Graphene. *J. Phys. Chem. C* **2010**, *114*, 16541.

(23) Kim, G.; Jhi, S.-H. Carbon Monoxide-Tolerant Platinum Nanoparticle Catalysts on Defect-Engineered Graphene. *ACS Nano* **2011**, *5*, 805.

(24) Kim, G.; Jhi, S.-H.; Park, N.; Louie, S. G.; Cohen, M. L. Optimization of Metal Dispersion and Hydrogen Adsorption Strength in Graphitic Materials for Hydrogen Storages. *Phys. Rev. B* **2008**, *78*, 085408.

(25) Kim, G.; Jhi, S.-H.; Lim, S.; Park, N. Crossover between Multipole Coulomb and Kubas Interactions in Hydrogen Adsorption on Metal−Graphene Complexes. *Phys. Rev. B* **2009**, *79*, 155437.

(26) Lee, C.; Wei, X.; Kysar, J. W.; Hone, J. Measurement of the Elastic Properties and Intrinsic Strength of Monolayer Graphene. *Science* **2008**, *321*, 385.

(27) Kim, K. S.; Zhao, Y.; Jang, H.; Lee, S. Y.; Kim, J. M.; Kim, K. S.; Ahn, J.-H.; Kim, P.; Choi, J.-Y.; Hong, B. H. Large-Scale Pattern Growth of Graphene Films for Stretchable Transparent Electrodes. *Nature* **2009**, *457*, 706.

(28) Kresse, G.; Furthmüller, J. Efficient Iterative Schemes for *Ab Initio* Total-Energy Calculations Using a Plane-Wave Basis Set. *Phys. Rev. B* **1996**, *54*, 11169.

(29) Kresse, G.; Joubert, D. From Ultrasoft Pseudopotentials to the Projector Augmented-Wave Method. *Phys. Rev. B* **1999**, *59*, 1758.

(30) Perdew, J. P.; Burke, K.; Ernzerhof, M. Generalized Gradient Approximation Made Simple. *Phys. Rev. Lett.* **1996**, *77*, 3865.

(31) Choi, S.-M.; Jhi, S.-H.; Son, Y.-W. Effects of Strain on Electronic Properties of Graphene. *Phys. Rev. B* **2010**, *81*, 081407.

(32) Choi, S.-M.; Jhi, S.-H.; Son, Y.-W. Controlling Energy Gap of Bilayer Graphene by Strain. *Nano Lett.* **2010**, *10*, 3486.

(33) Cretu, O.; Krasheninnikov, A. V.; Rodríguez-Manzo, J. A.; Sun, L.; Nieminen, R. M.; Banhart, F. Migration and Localization of Metal Atoms on Strained Graphene. *Phys. Rev. Lett.* **2010**, *105*, 196102.

(34) Jin, K.-H.; Choi, S.-M.; Jhi, S.-H. Crossover in the Adsorption Properties of Alkali Metals on Graphene. *Phys. Rev. B* **2010**, *82*, 033414.

(35) Chan, K. T.; Neaton, J. B.; Cohen, M. L. First-Principles Study of Metal Adatom Adsorption on Graphene. *Phys. Rev. B* **2008**, *77*, 235430.

(36) Kumar, V.; Kawazoe, Y. Evolution of Atomic and Electronic Structure of Pt Clusters: Planar, Layered, Pyramidal, Cage, Cubic, and Octahedral Growth. *Phys. Rev. B* **2008**, *77*, 205418.
(37) Cheng, X.; Shi, Z.; Glass, N.; Zhang, L.; Zhang, J.; Song, D.; Liu, Z.-S.; Wang, H.; Shen, J. A Review of PEM Hydrogen Fuel Cell Contamination: Impacts, Mechanisms, and Mitigation. *J. Power Sources* **2007**, *165*, 739.
(38) Zhang, S.; Yuan, X.-Z.; Hin, J. N. C.; Wang, H.; Friedrich, K. A.; Schulze, M. A Review of Platinum-Based Catalyst Layer Degradation in Proton Exchange Membrane Fuel Cells. *J. Power Sources* **2009**, *194*, 588.
(39) Bligaard, T.; Nørskov, J. K.; Dahl, S.; Matthiesen, J.; Christensen, C. H.; Sehested, J. The Brønsted−Evans−Polanyi Relation and the Volcano Curve in Heterogeneous Catalysis. *J. Catal.* **2004**, *224*, 206.
(40) Nørskov, J. K.; Bligaard, T.; Logadottir, A.; Bahn, S.; Hansen, L. B.; Bollinger, M.; Bengaard, H.; Hammer, B.; Sljivancanin, Z.; Mavrikakis, M.; et al. Universality in Heterogeneous Catalysis. *J. Catal.* **2002**, *209*, 275.
(41) Nørskov, J. K.; Bligaard, T.; Hvolbæk, B.; Abild-Pedersen, F.; Chorkendorff, I.; Christensen, C. H. The Nature of the Active Site in Heterogeneous Metal Catalysis. *Chem. Soc. Rev.* **2008**, *37*, 2163.
(42) Nørskov, J. K.; Bligaard, T.; Rossmeisl, J.; Christensen, C. H. Towards the Computational Design of Solid Catalysts. *Nat. Chem.* **2009**, *1*, 37.
(43) Jiang, T.; Mowbray, D. J.; Dobrin, S.; Falsig, H.; Hvolbæk, B.; Bligaard, T.; Nørskov, J. K. Trends in CO Oxidation Rates for Metal Nanoparticles and Close-Packed, Stepped, and Kinked Surfaces. *J. Phys. Chem. C* **2009**, *113*, 10548.
(44) Mills, G.; Jónsson, H.; Schenter, G. K. Reversible Work Transition State Theory: Application to Dissociative Adsorption of Hydrogen. *Surf. Sci.* **1995**, *324*, 305.